systematic methodology for trading off eigenvector placement vs gain magnitudes, while still maintaining desired closed-loop eigenvalue locations. An example demonstrated how solutions yielding achievable eigenvectors close to the desired eigenvectors could be obtained with significant reductions in gain magnitude compared to the direct eigenspace assignment solution. This result demonstrates how this method makes eigenspace assignment a much more practical and useful control-system synthesis method.

References

[1]Moore, B., "On the Flexibility Offered by State Feedback in Multivariable Systems Beyond Closed-Loop Eigenvalue Assignment," *IEEE Transactions on Automatic Control*, Vol. 21, Oct. 1976, pp. 689–692.

[2]Srinathkumar, S., "Eigenvalue/Eigenvector Assignment Using Output Feedback," NASA TP-1118, 1978.

[3]Fahmy, M., and O'Reilly, J., "On Eigenstructure Assignment in Linear Multivariable Systems," *IEEE Transactions on Automatic Control*, Vol. 27, No. 3, 1982, pp. 690–693.

[4]Andry, A., Shapiro, E., and Chung, J., "Eigenstructure Assignment for Linear Systems," *IEEE Transactions on Aerospace and Electronic Systems*, Vol. 19, No. 5, 1983, pp. 711–729.

[5]Davidson, J., Foster, J., Ostroff, A., Lallman, F., Murphy, P., Hoffler, K., and Messina, M., "Development of a Control Law Design Process Utilizing Advanced Synthesis Methods with Application to the NASA F-18 HARV," *High-Angle-of-Attack Projects and Technology Conf.*, NASA CP-3137, edited by N.W. Matheny, Vol. 4, NASA Dryden Flight Research Faculty, Edwards, CA, 1992, pp. 111–157.

[6]Davidson, J., and Andrisani, D., "Gain Weighted Eigenspace Assignment," NASA TM-109130, 1994.

[7]Graham, A., *Kronecker Products and Matrix Calculus: With Application*, Wiley, New York, 1981, Chap. 2.

[8]Fletcher, R., and Powell, M., "A Rapidly Convergent Descent Method for Minimization," *Computer Journal*, Vol. 6, July 1963, pp.163–168.

Command Shaping in Tracking Control of a Two-Link Flexible Robot

Arun K. Banerjee*
Lockheed Martin Advanced Technology Center, Palo Alto, California 94304
and
William E. Singhose†
Massachusetts Institute of Technology, Cambridge, Massachusetts 02139

I. Introduction

TRACKING of a periodic trajectory by a flexible multibody sensor is important in the fields of both spacecraft dynamics and robotics. In robotics, endpoint tracking control of a single flexible arm has been demonstrated by techniques such as adaptive control,[1] input-output inversion,[2] and time-optimal control.[3,4] An alternative technique, of control augmentation with input shaping,[5] is both simple and robust and has been shown to be effective in reducing vibrations during and after slewing[6,7] and in tracking.[8] Application of multimode input shaping to tracking control of nonlinear, flexible multibody systems has not been investigated previously. This Note considers such an application, with linear or nonlinear control of a two-link flexible robot where the endpoint of the robot is to track a periodic trajectory in minimum time in a repetitive manner.

Received Dec. 29, 1997; accepted for publication July 15, 1998.

*Consulting Scientist, Structures and Controls, H1-61/250. Associate Fellow AIAA.

†Postdoctoral Fellow, Mechanical Engineering Department; currently Assistant Professor, Mechanical Engineering Department, Georgia Institute of Technology, Atlanta, GA 30332. Member AIAA.

II. Modeling

Each beam of the two-link flexible robot is modeled as a series of rigid rods connected by rotational springs, where the spring coefficients are computed by equating deflections of a cantilever beam with those of the model due to a unit tip load. This Note uses the order-n formulation of the dynamical equations of Ref. 6. Each beam is broken into rigid segments interconnected by rotational springs. The order-n equations of motion for this n degree-of-freedom system are written in terms of the $(n \times 1)$ vector q of joint and elastic rotation angles and the (2×1) joint torque vector u as

$$\ddot{q} = f(\dot{q}, q, t) + b(q)u \tag{1}$$

where the equations, not reported here for brevity, are valid for small, as well as large, deflections of the flexible links. Equation (1) is a full-order flexible body model of the two-link robot, with two rigid and four elastic degrees of freedom. For control law design the links are treated as rigid. The equations of motion for the case when both links are rigid, of identical length L and mass m driven by joint torques T_1 and T_2, are of the form

$$[M(q)]\{\ddot{q}\} + C(\dot{q}, q, t) = T \tag{2}$$

where q is a (2×1) matrix of joint angles with elements q_1 and q_2; the functional dependencies are shown in parentheses, with the meaning

$$M = \begin{bmatrix} mL^2\left(\frac{5}{3} + \cos q_2\right) & mL^2\left(\frac{1}{3} + 0.5\cos q_2\right) \\ mL^2\left(\frac{1}{3} + 0.5\cos q_2\right) & mL^2/3 \end{bmatrix} \tag{3}$$

$$C = -(0.5mL^2 \sin q_2)\begin{bmatrix} \dot{q}_2(2\dot{q}_1 + \dot{q}_2) \\ -\dot{q}_1^2 \end{bmatrix} \tag{4}$$

$$T = \begin{Bmatrix} T_1 \\ T_2 \end{Bmatrix} \tag{5}$$

Now we consider independent joint control based on the reduced-order model of Eq. (2), so that measurement of beam deflections is not needed for the feedback control law.

III. Control and Inverse Kinematics

The method of feedback linearization[9] could be applied to Eq. (2), setting

$$T = M\left[\ddot{q}_c - 2\zeta\omega(\dot{q} - \dot{q}_c) - \omega^2(q - q_c)\right] + C \tag{6}$$

where M and C are given by Eqs. (3) and (4). Equation (6) ensures asymptotic decay of the tracking error. This is a model-based nonlinear control law with complex feedback. A simple linear control law can be derived from this, ignoring all coupling, with joint torques given by feedforward plus proportional-derivative feedback:

$$T_1 = \left(\tfrac{8}{3}mL^2\right)\left[\ddot{q}_{1c} - \omega^2(q_1 - q_{1c}) + 2\zeta\omega(\dot{q}_1 - \dot{q}_{1c})\right] \tag{7}$$

$$T_2 = (mL^2/3)\left[\ddot{q}_{2c} - \omega^2(q_2 - q_{2c}) + 2\zeta\omega(\dot{q}_2 - \dot{q}_{2c})\right] \tag{8}$$

where ζ and ω are the closed-loop damping and bandwidth, respectively, for controlling a rigid-body inertia. Taking ω as the first open-loop system mode, i.e., $\omega = 8.21$ Hz (note that ω is not the bandwidth of the actual flexible-body system) and $\zeta = 0.707$, and putting Eqs. (7) and (8) into Eq. (1) yield the closed-loop poles for the flexible robot as $-0.014 \pm 7.38j$, $-0.85 \pm 16j$, -37.5, -65.7, $-0.46 \pm 89.8j$, $-13.3 \pm 120.9j$, -259.6, and $-11{,}178$.

In Eqs. (7) and (8) the commanded values of the joint angles q_1 and q_2 and their first and second derivatives are obtained from the inverse kinematics of this two-link rigid-body model. Given commanded endpoint locations of the robot in inertial frame components (x_c, y_c),

a closed-form solution for the joint angles can be obtained from geometry[9] as

$$\cos q_{2c} = \frac{x_c^2 + y_c^2 - 2L^2}{2L^2} \tag{9}$$

$$q_{1c} = \tan^{-1}\left(\frac{y_c}{x_c}\right) - \tan^{-1}\left(\frac{\sin q_{2c}}{1 + \cos q_{2c}}\right) \tag{10}$$

Given (x_c, y_c) as functions of time, commanded first and second derivatives of the joint angles may be obtained as follows:

$$\begin{Bmatrix} \dot{q}_{1c} \\ \dot{q}_{2c} \end{Bmatrix} = [J(q_{1c}, q_{2c})]^{-1} \begin{Bmatrix} \dot{x}_c \\ \dot{y}_c \end{Bmatrix} \tag{11}$$

$$\begin{Bmatrix} \ddot{q}_{1c} \\ \ddot{q}_{2c} \end{Bmatrix} = [J(q_{1c}, q_{2c})]^{-1} \left\{ \begin{pmatrix} \ddot{x}_c \\ \ddot{y}_c \end{pmatrix} - [\dot{J}(q_{1c}, q_{2c}, \dot{q}_{1c}, \dot{q}_{2c})] \begin{pmatrix} \dot{q}_{1c} \\ \dot{q}_{2c} \end{pmatrix} \right\} \tag{12}$$

where the elements of the Jacobian J, which is a 2×2 matrix for the rigid two-link robot model, are evaluated from Eqs. (9) and (10) by differentiation. It is assumed that the inverse of the Jacobian exists. In practice, singular configurations may occur near corners. Singularity avoidance schemes, such as by use of redundant manipulators, are discussed in the robotics literature and are not considered within the scope of this Note.

IV. Input Shaping

The input shaping control technique attempts to eliminate residual vibration by generating a command signal that is self-canceling, that is, any vibration induced by the command is canceled by a later portion of the command. Input shaping is implemented by the convolution of a sequence of impulses with the desired command. The result of the convolution is used to command the system. We elect to traverse a path in minimum time that, however, excites multiple vibration modes. The minimum time nominal solution is a bang-bang command in acceleration. This can be thought of as the result of a convolution of a step command and the following impulse sequence:

$$\begin{bmatrix} t_i \\ A_i \end{bmatrix} = \begin{bmatrix} 0 & t_f/2 & t_f \\ 1.0 & -2.0 & 1.0 \end{bmatrix} \tag{13}$$

where the switching occurs at the midpoint of the final time t_f for a given maximum acceleration. A robust input shaper that eliminates residual vibration and is insensitive to modeling errors in frequency has been shown by Singer and Seering[5] to be the three-impulse sequence

$$\begin{bmatrix} t_i \\ A_i \end{bmatrix} = \begin{bmatrix} 0 & T/2 & T \\ 0.25 & 0.5 & 0.25 \end{bmatrix} \tag{14}$$

where the vibration mode to suppress is of period T. By convolving the sequences in Eqs. (13) and (14), we obtain

$$\begin{bmatrix} t_i \\ A_i \end{bmatrix} = \begin{bmatrix} 0.0 & T/2 & T & t_f/2 & (T+t_f)/2 & T+t_f/2 & t_f & t_f+T/2 & t_f+T \\ 0.25 & 0.75 & 1.0 & 0.5 & -0.5 & -1.0 & -0.75 & -0.25 & 0.0 \end{bmatrix} \tag{15}$$

The sequence in Eq. (15) is further convolved with a step function in the acceleration to get the desired command necessary to suppress a target mode of period T. A similar procedure is used to robustly suppress vibration in two modes of periods T_1 and T_2, for which the impulse sequence analogous to Eq. (15) is

$$\begin{bmatrix} t_i \\ A_i \end{bmatrix} = \begin{bmatrix} 0.0 & T_2/2 & T_2 & T_1/2 & (T_1+T_2)/2 & T_2+T_1/2 & T_1 & T_1+T_2/2 & T_1+T_2 \\ \frac{1}{16} & \frac{1}{8} & \frac{1}{16} & \frac{1}{8} & \frac{1}{4} & \frac{1}{8} & \frac{1}{16} & \frac{1}{8} & \frac{1}{16} \end{bmatrix} \tag{16}$$

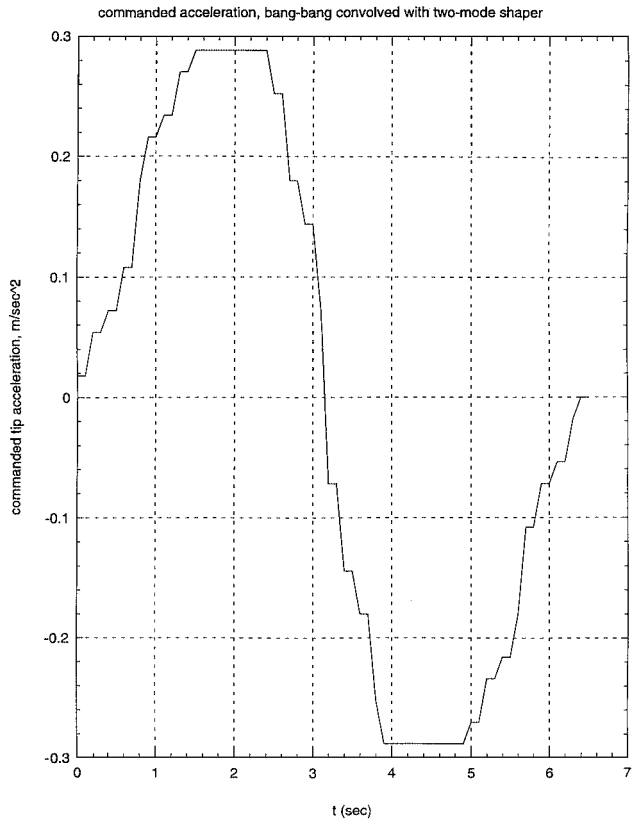

Fig. 1 Commanded tip bang-bang acceleration with input shaping for two modes.

V. Performance and Robustness

We consider a square trajectory to be tracked by the endpoint of the two-link flexible robot. This trajectory is challenging because the change in commanded direction at a corner of the square is likely to induce vibration. For the numerical simulation $n = 6$, each beam—of length 4.5 m, flexural rigidity 1676 N-m^2, and mass density 0.335 kg/m—is broken into three equal rigid elements, and the rotational springs connecting the pieces are of stiffness 1117.4 N-m/rad. The system elastic frequencies are 8.21, 8.56, 25.4, and 25.7 Hz. Simulation of tracking control of a prescribed square trajectory for the endpoint of the two-link flexible manipulator has been done with all tracking starting at the lower left corner of a square. Minimum travel time t_f giving a bang-bang command acceleration of 0.288 m/s^2 in rest-to-rest motion along a side of length 1.8 m was taken as 5.0 s. Figure 1 shows the two-mode shaper to eliminate two closed-loop modes, of period 0.85 and 0.40 s, for x- and y-direction accelerations. Figure 2 shows the results of using the nonlinear control law, Eq. (6), with and without input shaping, and the effect of input shaping in suppressing vibrations is clear. Similar results[10] are obtained with the linear control law, Eqs. (7) and (8), and the results of three repetitive executions of the trajectory when the control is used with and without any input shaping are shown in Fig. 3. The smear in the figure for the contour tracked is due to cumulative error buildup without input shaping when terminal errors in position and velocity in any segment of the track are nonzero. The straight-sided rectangle in Fig. 3 represents the improvement

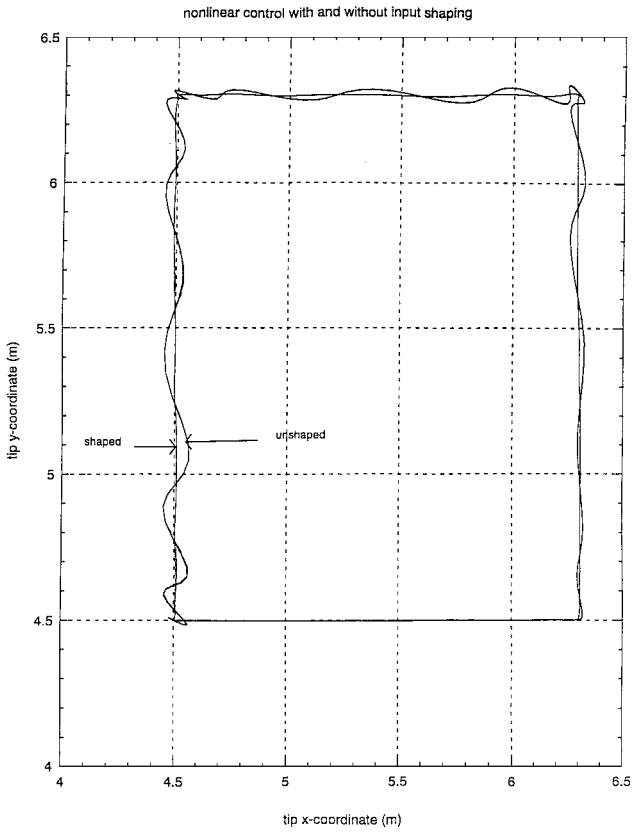

Fig. 2 Nonlinear tracking control with and without input shaping.

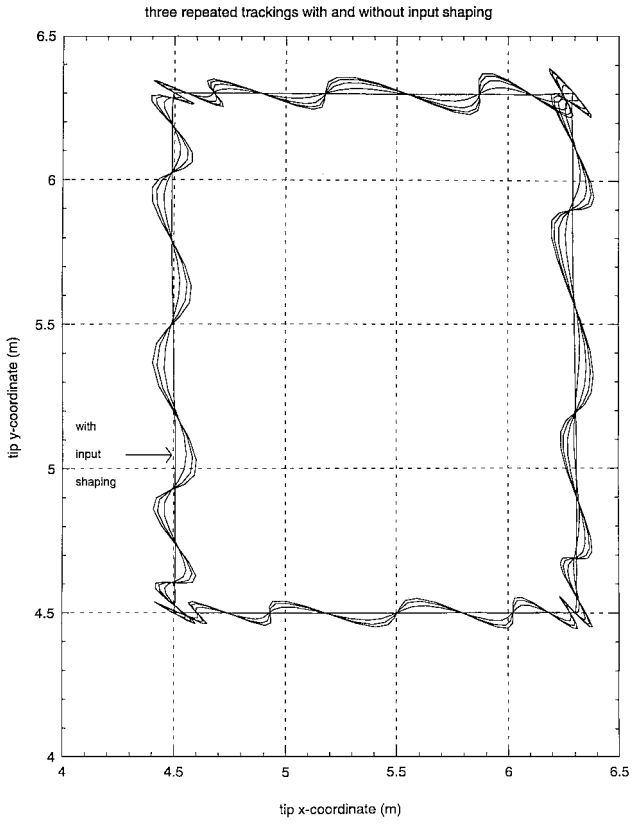

Fig. 3 Linear control with and without input shaping for repetitive tracking.

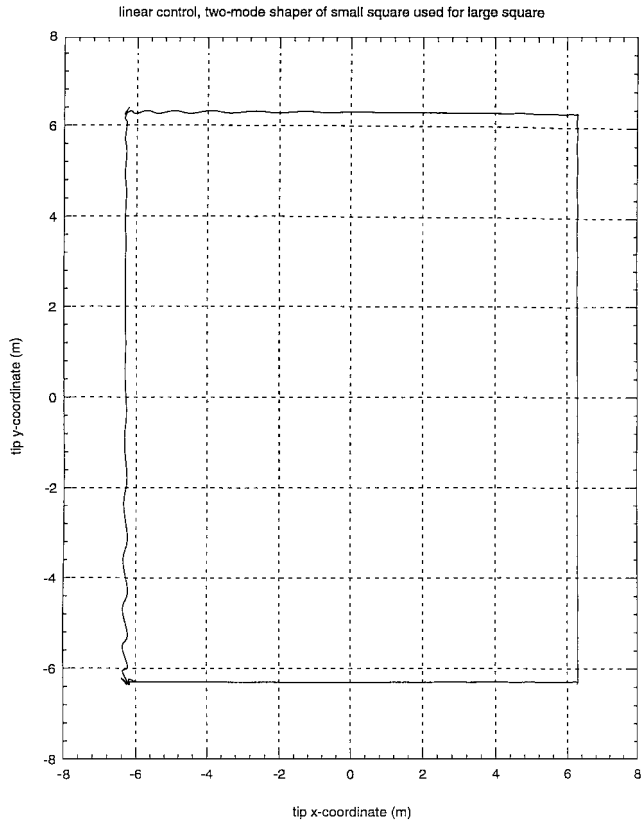

Fig. 4 Linear control with input shaping, with gains for tracking a small square used in tracking a large square.

attained for the same three repetitive trackings with input shaping, where linear control with two-mode shaping causes very little smear.

Robustness of the input shaped tracking controller can be examined by changing the desired trajectory. To this end we consider tracking a much larger square, with each side of length 12.6 m covered in a rest-to-rest motion with the same maximum acceleration as before, namely, 0.288 m/s^2. Using the same control laws and the same input shaping as that used for tracking the smaller square, one obtains for the larger square the results for linear control with two-mode shaping, given in Fig. 4. The eigenvalues of the closed-loop plant about the initial configuration, in the lower left corner of the square, are $-0.017 \pm 5.42j$, $-0.85 \pm 25.9j$, -37.5, -43.8, $-1.5 \pm 79.9j$, $-2.1 \pm 130.2j$, -1131.4, and $-11{,}217$.

This shows that the first two closed-loop modes for this new configuration are of period 1.16 and 0.24 s, compared with 0.85 and 0.4 s obtained for the initial configuration corresponding to the lower left corner of the smaller square. In the light of the mistuning, the performance degradation in Fig. 4 is to be expected, and one could reasonably conclude that the control scheme is robust.

VI. Conclusion

Endpoint tracking control performance of a two-link flexible robot has been shown to be improved with input shaping based on the vibration modes of the actual closed-loop system, using either a nonlinear or a linear control law based on a rigid-body model of the system. It is shown that input shaping of closed-loop control modes gives a robust performance, and it greatly improves repetitive tracking of a space-fixed trajectory.

References

[1]Sasiadek, J. Z., and Srinivasan, R., "Dynamic Modeling and Adaptive Control of a Single-Link Flexible Manipulator," *Journal of Guidance, Control, and Dynamics*, Vol. 12, No. 6, 1989, pp. 838–844.

[2]De Luca, A., and Siciliano, B., "Trajectory Control of a Nonlinear One-Link Flexible Arm," *International Journal of Control*, Vol. 50, No. 5, 1989, pp. 1699–1715.

[3]Pao, L. Y., "Minimum-Time Control Characteristics of Flexible Structures," *Journal of Guidance, Control, and Dynamics*, Vol. 19, No. 1, 1996, pp. 123–129.

[4]Singh, T., and Vadali, S. R., "Robust Time-Optimal Control: A Frequency Domain Approach," *Journal of Guidance, Control, and Dynamics*, Vol. 17, No. 2, 1994, pp. 346–353.

[5]Singer, N. C., and Seering, W. P., "Preshaping Command Inputs to Reduce System Vibration," *Journal of Dynamic Systems, Measurement and Control*, Vol. 12, March 1990, pp. 76–82.

[6]Banerjee, A. K., "Dynamics and Control of the Shuttle-Antennae System," *Journal of the Astronautical Sciences*, Vol. 41, Jan.–March, 1993, pp. 73–90.

[7]Singhose, W., Banerjee, A. K., and Seering, W. E., "Slewing Flexible Spacecraft with Deflection Limiting Input Shaping," *Journal of Guidance, Control, and Dynamics*, Vol. 20, No. 2, 1997, pp. 291–298.

[8]Singhose, W., and Singer, N., "Effects of Input Shaping on Two-Dimensional Trajectory Following," *IEEE Transactions on Robotics and Automation*, Vol. 12, No. 6, 1996, pp. 881–887.

[9]Spong, M. W., and Vidyasagar, M., *Robot Dynamics and Control*, Wiley, New York, 1989, pp. 24, 259–283.

[10]Banerjee, A. K., and Singhose, W. E., "Input Shaping with Nonlinear Tracking Control of a Two-Link Flexible Robot," AAS/AIAA Astrodynamics Specialist Conf., AAS Paper 97-121, Sun Valley, ID, Aug. 1997.

Simple Guidance Scheme for Low-Thrust Orbit Transfers

Craig A. Kluever*
University of Missouri–Columbia
Kansas City, Missouri 64110

Introduction

SPACE missions using solar electric propulsion (SEP) will, it is hoped, become more commonplace after SEP technology is successfully demonstrated by the first new millennium mission, Deep Space 1. Much of the previous low-thrust flight mechanics research has been devoted to computing optimal (minimum-fuel or minimum-time) trajectories. Examples include transfers from low Earth orbit (LEO) to geosynchronous orbit (GEO).[1–3] By comparison, the volume of work on guidance laws for electric propulsion spacecraft is somewhat limited. Early examples of low-thrust guidance schemes for lunar and interplanetary missions are presented by Battin[4] and Breakwell and Rauch,[5] respectively. More recent low-thrust guidance methods are demonstrated in Refs. 6–8.

Trajectory optimization methods often utilize a calculus of variations approach, which obtains the optimal trajectory by solving a corresponding two-point boundary-value problem (TPBVP). As a result of the TPBVP solution, the Euler–Lagrange or costate equations define the thrust vector steering control during the optimal transfer in an open-loop fashion. For realistic onboard guidance schemes, the implementation of the optimal control defined by the costate equations may not be feasible or practical for the very long duration transfers performed by low-thrust spacecraft. For example, a typical LEO–GEO transfer using SEP would require hundreds of days of continuous thrusting and thousands of revolutions. This presents several challenges for designing a guidance system for steering the thrust vector. In addition, the level of ground support is significantly increased if frequent uplinks of new guidance commands for thrust steering is necessary. Therefore, a simple autonomous guidance scheme (which can be easily stored and implemented on board the spacecraft) that provides near-optimal performance would be highly beneficial for low-thrust mission operations.

Presented as Paper 98-203 at the AAS/AIAA Space Flight Mechanics Meeting, Monterey, CA, Feb. 9–11, 1998; received May 4, 1998; revision received June 22, 1998; accepted for publication July 1, 1998.

*Assistant Professor, Mechanical and Aerospace Engineering Department. Senior Member AIAA.

This Note presents a simple guidance scheme for performing low-thrust orbital transfers. The guidance is based on optimal control laws that are developed by investigating the nature of the variational equations for the orbital elements. The individual control laws are blended so that a simultaneous change of several orbit elements is enacted. A numerical simulation of a low-thrust LEO–GEO transfer is presented to demonstrate the proposed guidance scheme.

Guidance Scheme

Control Laws

The proposed guidance method is based on a combination of individual optimal control laws that maximize the time rate of change of a desired orbital element. To demonstrate the foundation of the optimal controls, the governing differential equations for semimajor axis a, eccentricity e, and inclination i are presented:

$$\frac{da}{dt} = \frac{2a^2 v}{\mu} a_T \cos\phi \tag{1}$$

$$\frac{de}{dt} = \frac{a_T}{v}\left[2(e+\cos\nu)\cos\phi + \frac{r}{a}\sin\nu\sin\phi\right] \tag{2}$$

$$\frac{di}{dt} = \frac{a_T r}{h}\cos\theta\sin\beta \tag{3}$$

where v is the velocity magnitude, a_T is the thrust acceleration magnitude (thrust/mass), μ is the gravitational constant, h is the angular momentum, r is the radial position magnitude, ν is the true anomaly, ω is the argument of periapsis, and $\theta = \omega + \nu$. The in-plane thrust-steering angle ϕ is measured from the velocity vector to the projection of the thrust vector onto the orbit plane, and the out-of-plane (yaw) steering angle β is measured from the orbit plane to the thrust vector. The optimal controls $\phi_a^*(t)$, $\phi_e^*(t)$, and $\beta^*(t)$ are derived from the first-order necessary (stationarity) condition for optimality for each respective variational equation [e.g., $\phi_a^*(t)$ satisfies $\partial\dot{a}/\partial\phi = 0$, etc.]. The optimal controls that maximize da/dt, de/dt, and di/dt are

$$\phi_a^* = 0 \tag{4}$$

$$\tan\phi_e^* = \frac{r\sin\nu}{2a(e+\cos\nu)} \tag{5}$$

$$\beta^* = (\pi/2)\mathrm{sgn}(\cos\theta) \tag{6}$$

The preceding controls maximize the respective variational equations because the second-order sufficient condition check yields negative values (e.g., $\partial^2\dot{a}/\partial\phi^2 < 0$). Although Eq. (6) is the optimal steering law for maximizing di/dt, any out-of-plane steering is essentially wasted when the longitude angle θ is near ± 90 deg. Therefore, the yaw steering law

$$\beta^* = (\pi/2)\cos\theta \tag{7}$$

provides a good feedback steering law for near-maximum $+di/dt$ and does not waste the thrust force near $\theta = \pm 90$ deg.

Blending the Control Laws

The in-plane thrust steering is obtained by blending the in-plane optimal controls (4) and (5). The basic steps are as follows:

1) Compute the unit vectors $\boldsymbol{c}_a$ and $\boldsymbol{c}_e$ that define the in-plane optimal controls for maximum da/dt and de/dt, respectively. The unit vectors are expressed in a local rotating radial-transverse-normal (*RTN*) coordinate frame where the R axis is along the radial direction, the T axis is in the orbit plane along the transverse direction, and the N axis is normal to the orbit plane (however, the in-plane steering unit vectors $\boldsymbol{c}_a$ and $\boldsymbol{c}_e$ will only have R and T components). A general expression for the unit vector in the *RTN* frame is

$$\boldsymbol{c}_k = \left[\sin\left(\gamma + \phi_k^*\right), \cos\left(\gamma + \phi_k^*\right), 0\right]^T, \qquad k = a, e \tag{8}$$

where ϕ_a^* and ϕ_e^* are computed using the optimal controls (4) and (5). The angle γ is the flight-path angle and is measured from the local horizon to the velocity vector.